



Contents lists available at ScienceDirect

Bioorganic & Medicinal Chemistry Letters

journal homepage: www.elsevier.com/locate/bmclDiscovery of potent and selective PPAR α / δ dual antagonists and initial biological studies

Jason D. Jacintho*, Christopher S. Baccei, Yalda Bravo, Alex Broadhead, Austin Chen, Lucia Correa, Kim Fischer, Bryan Laffitte, Catherine Lee, Daniel S. Lorrain, Davorka Messmer, Peppi Prasit, Karin J. Stebbins, Nicholas S. Stock

Inception Sciences, Suite 100, 5871 Oberlin Drive, San Diego, CA 92121, USA

ARTICLE INFO

Keywords:

PPAR alpha
PPAR delta
Antagonist
Small molecule
Cancer

ABSTRACT

We previously published on the design and synthesis of novel, potent and selective PPAR α antagonists suitable for either i.p. or oral *in vivo* administration for the potential treatment of cancer. Described herein is SAR for a subsequent program, where we set out to identify selective and potent PPAR α / δ dual antagonist molecules. Emerging literature indicates that both PPAR α and PPAR δ antagonism may be helpful in curbing the proliferation of certain types of cancer. This dual antagonism could also be used to study PPARs in other settings. After testing for selective and dual potency, off-target counter screening, metabolic stability, oral bioavailability and associated toxicity, compound **11**, the first reported PPAR α / δ dual antagonist was chosen for more advanced preclinical evaluation.

Introduction

In our previous publications,^{1,2} we identified, to the best of our knowledge, the first selective PPAR α antagonists suitable for advanced *in vivo* preclinical studies. PPAR α , one of three distinct PPAR (peroxisome proliferator-activated receptor) isoforms (α , δ and γ) is largely responsible for the regulation of lipid metabolism. Agonism of PPAR α is known to facilitate fatty acid oxidation (FAO), so we hypothesized that antagonism of PPAR α would be a useful probe to study in certain fatty acid (FA) metabolizing cancer cells, including: ovarian,³ renal cell carcinoma,⁴ and certain types of detached metastatic cells.^{5–7}

PPAR δ , together with PPAR α , are critical in the sensing of fatty acid levels and each is central to the cascade of FA-induced gene expression.⁸ All three PPAR isoforms are highly homologous, but they differ in terms of their respective tissue distribution as well as ligand specificity. Whereas PPAR α is primarily expressed in tissues with a propensity for extensive FA catabolism, e.g, liver, heart, kidney and skeletal muscle, PPAR δ is ubiquitously expressed.⁹ We hypothesized that a dual PPAR α / δ antagonist may prove superior to PPAR α inhibition alone by virtue of potential overlap in their inherent functions. It was recently revealed that inhibitors of the PPAR-mediated FAO pathway could be useful in treating resistant breast cancer,¹⁰ glioblastoma,¹¹ and the clearance of quiescent leukemia initiating cells.⁸ Inhibition of PPAR δ initiates cellular symmetric commitment pathways that result in the exhaustion of cancer stem cells. PPAR δ , in addition to its role in lipid and energy

metabolism, is implicated in other processes involving survival, proliferative genes,⁵ and angiogenesis.¹⁰ Publications have shown that PPAR δ antagonism,¹² and PPAR δ murine knockout models,¹³ slow down certain kinds of tumor progression. Corroborating evidence indicates that the converse is true, namely that PPAR δ agonists promote cancer cell proliferation and inhibit apoptosis.¹² More recent literature has suggested that suppression of PPAR δ could be useful against metastatic melanoma,¹⁴ and colon cancer.¹⁵ Finally, there is additional evidence that implicates PPARs in the regulation of multi-drug resistance proteins.¹⁶ It is possible that antagonizing one or more of the PPAR isoforms could reduce drug efflux and subsequent chemo-resistance.

It was our plan to identify a single molecule that would selectively antagonize both PPAR α and δ , in the hope that we would recruit an additive biological effect. It is worth mentioning that, as far as we are aware, no dual PPAR α / δ , single-agent antagonists have been reported to date. A challenging aspect of this endeavor is that the PPAR α and PPAR δ isoforms often bind to natural ligands of dissimilar structure.¹⁷ However, dual agonists of PPAR α / δ have been identified and proved to be good starting points for our SAR initiatives.¹⁸ Compound **1** (Fig. 1), a dual PPAR α / δ agonist, was our reference scaffold from which we based our initial derivatives. We tested whether a replacement of the fibrate carboxylic acid with an acylsulfonamide would trigger a literature-precedented PPAR agonist-to-antagonist switch (compounds **3** and **4**,

* Corresponding author.

E-mail address: jjacintho@inceptionsci.com (J.D. Jacintho).

<https://doi.org/10.1016/j.bmcl.2018.12.045>

Received 31 August 2018; Received in revised form 28 November 2018; Accepted 3 December 2018

0960-894X/© 2018 Elsevier Ltd. All rights reserved.

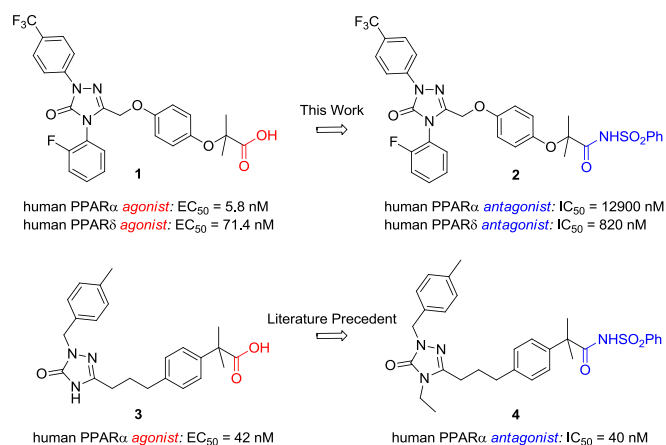


Fig. 1. Initial Probe of Fibrate Agonist to Acylsulfonamide Antagonist Switch.

Fig. 1).^{1,9}

We synthesized compound **2** with the hope of quickly achieving dual antagonism. This effort was only partly successful in that **2** is a moderately potent PPAR δ antagonist (IC₅₀ = 820 nM), but had little effect on the PPAR α isoform. It was at this point that we decided to completely replace the fibrate residue of **1**. We have previously identified and described the chemistry of several chemical functionalities which induce potent PPAR α antagonism when grafted on to known agonist scaffolds.^{1,2} We synthesized several of these antagonism-inducing fibrate replacements and their dual PPAR α and δ inhibitory potencies are listed in Table 1.

This initial effort (compounds **3–7**), in which potencies were obtained from standard PPAR α and δ luciferase cell-based functional assays,¹⁹ failed to identify a PPAR α / δ dual antagonist of ample potency. We did, however, succeed in making a potent and selective PPAR α inhibitor in compound **5**.

Table 1

PPAR α / δ dual antagonism of various fibrate replacements.

Compound	R	PPAR α IC ₅₀ ^a (μ M)	PPAR δ IC ₅₀ ^a (μ M)
3		31.44	1.97
4		38.14	3.74
5		0.018 ^b	> 100.0 ^c
6		11.44	4.49
7		30.99	48.80

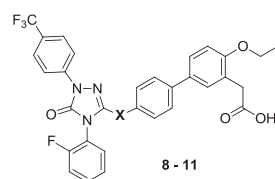
^a Values are the mean of at least three experiments except where noted.

^b Values are the mean of two experiments.

^c One experiment.

Table 2

PPAR α / δ dual antagonism: Replacement of the methoxy linker.



Compound	X	PPAR α IC ₅₀ ^a (μ M)	PPAR δ IC ₅₀ ^a (μ M)
8		1.10	0.319
9		0.424	0.667
10		23.12 ^b	27.73
11		0.113	0.025

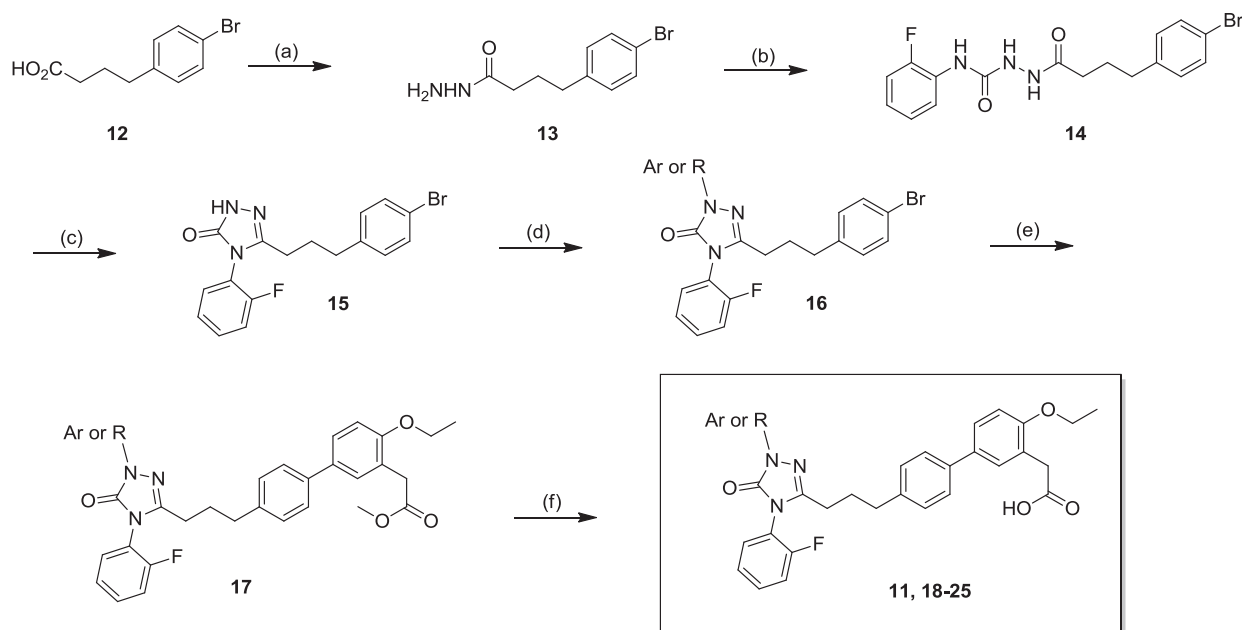
^a Values are the mean of at least three experiments except where noted.

^b Values are the mean of two experiments.

Next, we turned our attention toward the ether linker between the triazolone ring and the central phenyl ring. Compounds **8–11** (Table 2) were prepared in order to vary the length and composition of this linker moiety. For purposes of comparison, we kept the 2-ethoxyphenylacetic acid fibrate replacement found in compound **6** because it provided a balanced inhibition of both PPAR α and δ . To our gratification, extending the two-atom, methoxy linker to a three atom linker improved PPAR α / δ dual antagonism tremendously. In particular, compound **11**, with a three-carbon propyl chain, showed superior dual antagonism.

We built upon this discovery by making single-point substitutions on the triazolone ring, starting with the nitrogen at the 1-position. The general synthesis for making these derivatives is illustrated in Scheme 1. Commercially available butanoic acid **12**, was converted to acylhydrazide **13** via CDI coupling with hydrazine. Subsequent treatment with 2-fluorophenyl isocyanate afforded semicarbazide **14**, which was then cyclized to triazolone **15** with TMSOTf and triethylamine in refluxing toluene. The 1-position can then be diversified by alkylation or arylation using the desired alkyl bromide and cesium carbonate in acetonitrile or Ullmann conditions with the desired aryl iodide, respectively. These conditions provided aryl bromide intermediate **16** which was then coupled to methyl 2-(2-ethoxy-5-(4,4,5,5-tetramethyl-1,3,2-dioxaborolan-2-yl)phenyl)acetate under palladium-mediated Suzuki-Miyaura borylation conditions to provide the phenylacetic acid methyl ester **17**. Finally, hydrolysis of the ester provided the phenyl acetic acids **18–25** (Table 3).

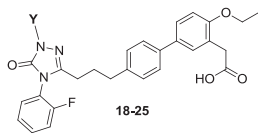
Upon examination of the SAR in Table 3, it should be stated that our effort here was not exhaustive by any means. We were working with an established SAR from a previous, related program.² In that work, most changes to the 1-position were detrimental to potency. We wanted to justify this bias with a representative, yet small number of analogs. Analysis of PPAR α / δ potencies in Table 3 reveal that no replacements were identified which were superior to the 4-trifluoromethylphenyl group found in **11**. Compound **18**, containing a small ethyl group at the 1-position, completely abrogated PPAR α antagonism and decreased that of PPAR δ by 280 fold. Moving the trifluoromethyl group to the 3-position, as in **19**, caused significant loss in potency across the two isoforms. Interestingly, compound **20** and **21**, each bearing substitutions similar to, yet slightly > **11**, had better potency on PPAR α , but were inferior on PPAR δ . We then screened a few sulfur-containing compounds, **22** and **23**, focusing in on what we assumed to be the privileged spot on the phenyl ring, the para-position. In general, neither of these compounds qualified as a dual antagonist of sufficient potency, but it was interesting that **22** appeared to be our first moderately



Scheme 1. (a) CDI, THF, RT then $\text{NH}_2\text{NH}_2 \cdot \text{H}_2\text{O}$, RT, 95%. (b) 2-Fluorophenyl NCO, THF, RT, > 99%. (c) TMSOTf, TEA, Tol, reflux. (d) ArI, CuI, *trans*-1,2-dimethylaminocyclohexane, K_2CO_3 , dioxane, reflux, ~30–90% (two step yield) or RBr, Cs_2CO_3 , CH₃CN, 50 °C, ~50–90% (two step yield). (e) Tetrakis(triphenylphosphine)palladium(0), methyl 2-(2-ethoxy-5-(4,4,5,5-tetramethyl-1,3,2-dioxaborolan-2-yl)phenyl)acetate, dioxane, sat. aq. NaHCO_3 , 85 °C, ~40–80%. (f) LiOH, THF, MeOH, H_2O , RT, ~90%.

Table 3

N-1 substitution: Effect on PPAR α / δ dual antagonism.



Compound	Y	PPAR α IC ₅₀ (μM) ^a	PPAR δ IC ₅₀ (μM) ^a
18		89.30 ^b	24.97
19		0.678	3.59
20		0.033	0.610
21		0.018	0.197
22		1.24	0.079
23		5.04	2.78
24		0.200	25.55
25		0.394	22.23

^a Values are the mean of at least three experiments except where noted.

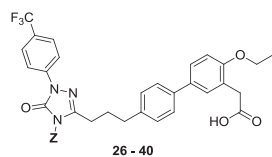
^b Value was obtained from one experiment.

selective PPAR δ antagonist. Finally, compounds 24 and 25 were synthesized to see what impact larger, single-carbon homologs had on potency. As the data reveals, neither of these compounds qualified as a dual inhibitor.

At this stage, we were satisfied that the 4-trifluoromethylphenyl group at position 1 of the triazolone was optimal. We then initiated what would be the most extensive portion of our PPAR α / δ dual antagonist SAR campaign. We hypothesized that replacement of the 2-fluorophenyl group at position 4 of the triazolone would give us the best chance to improve on compound 11. The general synthesis for compounds in Table 4 mirror the synthesis found in Scheme 1, where we simply used a variety of isocyanates (most of them available commercially) in the second step to introduce novel functionalities at position 4. We began by synthesizing alkyl groups of various sizes, as exemplified in compounds 26–29. The general trend seen here, in terms of dual potency, indicates that smaller groups boosted PPAR α inhibition to the detriment of PPAR δ potency. Compound 29 showed promising dual PPAR α / δ potency but was not selected for further evaluation due to borderline CYP3A4 induction potential (Table 5). Next, we made a variety of phenyl analogs, varying both the functionality and position of substitution. Compounds 30–36 were prepared and tested for dual potency. We were pleased to see that two of the compounds were either superior or better balanced, in terms of dual potency, when compared to compound 11. Whereas compound 30 was superior for inhibition of both PPAR isoforms, compound 36 was approximately five times more potent on PPAR α with only a small sacrifice in PPAR δ potency. Overall, it can be argued that both compound 30 and 36 were more balanced in terms of dual potency compared to 11. This excitement was proven premature as compound 30 showed significant CYP3A4 induction (Table 5) and compound 36 showed disappointing oral exposure in rat (data not shown) when compared to compound 11. Finally, we prepared several pyridyl analogs as replacements for the 2-fluorophenyl group (37–39) as well as a slightly larger, 2-fluorobenzyl homolog (40). All three pyridine replacements were tolerated and showed appreciable dual antagonism, but none of them proved superior to compound 11 in terms of potency. Compound 40 demonstrated to us that larger substitutions at this position would most likely prove detrimental.

Compounds 41 and 42 were synthesized and tested for PPAR α / δ dual antagonism (Fig. 2). Compound 41 was prepared in order to assess whether a simple switch of the two phenyl groups found on 11 would be tolerated. As the potency numbers show, this switch was detrimental

Table 4
N-4 substitution: Effect on PPAR α / δ dual antagonism.



Compound	Z	PPAR α IC ₅₀ (μ M) ^a	PPAR δ IC ₅₀ (μ M) ^a
26		0.051	0.438
27		0.032	0.439
28		0.055	0.124
29		0.066	0.066
30		0.023	0.018
31		0.216	0.030
32		0.021	0.138
33		0.080	0.040
34		0.420	0.083
35		0.433	0.515
36		0.017	0.034
37		0.569	0.047
38		0.126	0.061
39		0.122	0.225
40		0.608	1.62

^a Values are the mean of at least three experiments.

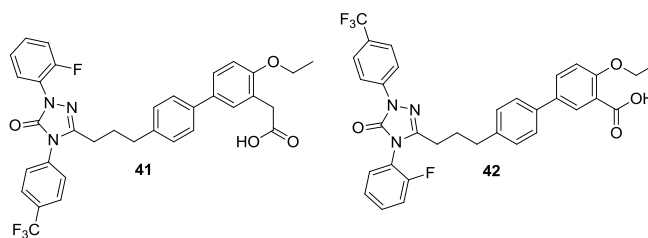
Table 5
CYP induction of selected compounds.

Compound	CYP Induction @ 10 μ M; % activity vs. 10 μ M Rifampicin ^a	CYP3A4 mRNA increase vs. Rifampicin ^b
11	19.7	21%
29	7.7	83%
30	55.7	204%

^a Average of 3 different donors.

^b 10 μ M solutions of each compound were compared to 10 μ M of Rifampicin and values are expressed as percentage vs. Rifampicin-induced mRNA increase.

to potency on both isoforms. Benzoic acid **42** was prepared because this class had proven to be very potent in previous stages of the project. As a dual inhibitor, **42** was nearly as potent as **11**, with the exception that



human PPAR α antagonist: IC₅₀ = 725 nM
human PPAR δ antagonist: IC₅₀ = 1240 nM

human PPAR α antagonist: IC₅₀ = 56 nM
human PPAR δ antagonist: IC₅₀ = 131 nM

Fig. 2. Additional analogs: Swapping of triazolone substituents (**41**). Benzoic acid analog (**42**).

Table 6
Screening summary for Compound **11**.

Assay Target	IC ₅₀ (μ M) ^a
PPAR α	0.113
PPAR δ	0.025
PPAR γ	21.3
PPAR α agonism	> 30 ^b
PPAR δ agonism	> 30 ^b
PPAR γ agonism	> 30
mousePPAR α	1.28
mousePPAR δ	0.96
mousePPAR γ	18.3
Estrogen Receptor β	10.4
Glucocorticoid Receptor	22.3
Thyroid Receptor	32.4
Retinoid X Receptor	24.4
PXR activation	Tested ^c
CYP3A4	> 30
CHO Cell Viability	> 30
CYP2C9	8.2
CYP2D6	> 30
CYP2C19	> 30
CYP1A2	> 30
CYP3A4 TDI	0.004 min ⁻¹
hERG	-4.1% @ 10 μ M

^a Values are the mean of at least three experiments except where noted.

^b Values are the mean of at least two experiments.

^c Moderate PXR activation at 10 μ M (56% of positive control Rifampicin) and no observed activation at 1 μ M.

the individual PPAR α and δ potencies were now switched in magnitude. Further consideration of compound **42** was terminated due to poor oral exposure in rats (data not shown).

Though we succeeded in synthesizing compounds which were superior or at least competitive with compound **11** in terms of dual PPAR α / δ inhibition, inferior DMPK attributes precluded their further development. Compound **11** was chosen for more advanced evaluation and proof-of-concept studies because of its superior profile (Table 6). When the sodium salt of compound **11** was orally administered as a 0.5% methocel solution at a dose of 10 mpk in rat, we observed good drug exposure with a calculated plasma AUC of 14.2 μ g^{*}h/mL. Detailed information for rat and dog oral and i.v. dosing is presented in Table 7.

Table 7
Pharmacokinetic^a Profile of Compound **11** in rats and dogs.

Species	%F	T _{1/2} i.v. (h)	C _{max} (μ g/mL)	AUC _{po} (h [*] μ g/mL)	Cl (mL/min/kg)	V _{DSS} (L/kg)
Rat	33.1	1.7	2.4	14.2	4.0	0.5
Dog	57.6	2.1	4.8	11.9	4.1	0.5

^a Compound was dosed at 2 mg/kg i.v. (water) and 10 mg/kg p.o. (0.5%) methylcellulose in rat and 2 mg/kg i.v. (saline) and 5 mg/kg p.o. (0.5%) methylcellulose in dog.

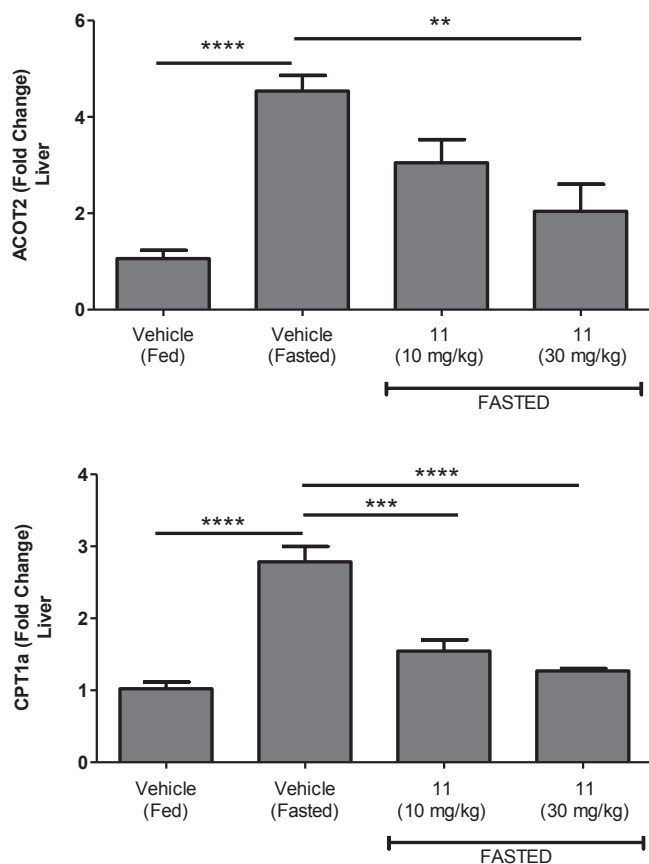


Fig. 3. PPAR gene attenuation in mouse livers. ACOT2 and CPT1a for Compound 11.

These exposures will be used to guide future toxicity studies.

Given the favorable *in vitro* profile of **11** and suitable pharmacokinetics, we wanted to evaluate its role in certain murine cancer models. In order to determine the efficacious dose, an *in vivo* target engagement study was designed.²⁰ Compound **11** was administered orally to mice at 10 and 30 mg/kg for 4 days. Mice were fasted for 48 h prior to sacrifice to induce PPAR regulated genes. Fasting significantly induced liver gene expression (Fig. 3) of ACOT2 (4.3-fold, $p < .0001$) and CPT1a (2.7-fold, $p < .0001$). This increase was dose responsively attenuated in animals treated with compound **11** at the 30 mg/kg dose. Relative to higher species, where we saw good systemic exposure upon oral dosing, higher dosing of compound **11** was anticipated in mice due to relatively low systemic exposures ($AUC_{po} \sim 2.9 \text{ h} \cdot \mu\text{g}/\text{mL}$, 10 mg/kg in 0.5% methylcellulose) in addition to poorer intrinsic potency in mouse PPARs (Table 6).

With target engagement and related systemic exposures in hand, we next evaluated the ability of compound **11** to impart protective benefits in two different tumor models at 30 mg/kg. First, we employed an experimental model of metastasis using the B16F10 cell line. It is postulated that detached metastatic cells, resistant to anoikis, undergo a radical shift in metabolism in order to survive.²¹ Non-glycolytic pathways, especially FAO, become important energy alternatives. Perturbation of FAO via PPAR antagonism should reduce the survivability of cancer cells in this model. As is evident from Fig. 4, compound **11** significantly attenuated the number of lung nodules compared to vehicle treated animals when orally dosed.²²

We also analyzed the ability of compound **11** to inhibit the growth of SKOV-3, a human ovarian cancer cell line (Fig. 5). It has been established that ovarian cancer cells rely extensively on FAO for energy due to an adipocyte-rich microenvironment.²³ Oral administration of **11** significantly inhibited the growth of these tumors over a 28 day

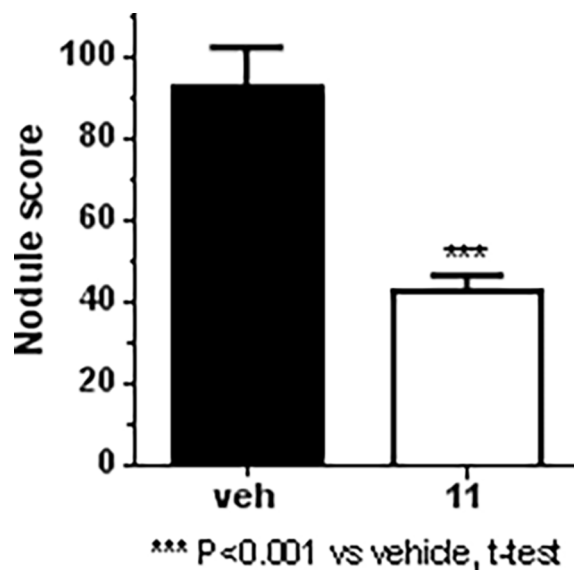


Fig. 4. B16F10 experimental metastasis model – Compound 11.

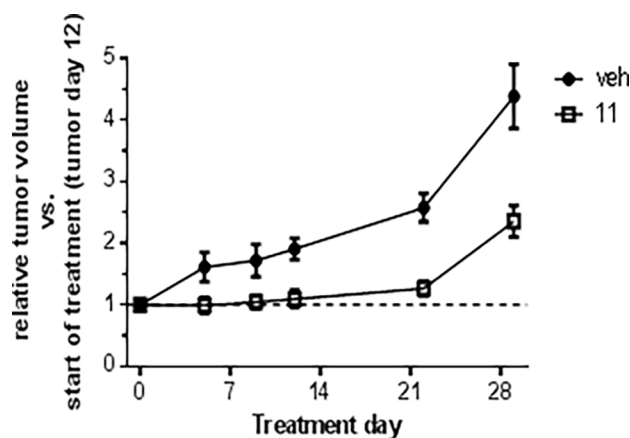


Fig. 5. SKOV-3 experimental xenograft model – Compound 11.

study period.²⁴ These two preliminary *in vivo* studies are certainly limited in scope as we were unable to determine the differences between engaging the host (mouse) PPARs versus human tumor cell PPARs. There are future plans for testing the differences between these two. We also plan to test compound **11** in other cancer models.

In summary, we have, to the best of our knowledge, designed and synthesized the first series of potent and selective PPAR α / δ dual antagonists that are suitable for *in vivo* proof-of-concept experiments. Use of previous SAR, which uncovered PPAR antagonist fibrates surrogates enabled us to rapidly identify compound **11** while synthesizing only a small library of compounds. With this selective tool in hand, it is now possible to more clearly elucidate the impact of simultaneous antagonism of PPAR α and PPAR δ in various assays including certain types of cancer. We will be reporting additional findings in this regard in due course.

Acknowledgements

We would like to thank Lisa Rahbaek and Diem Vo for their contributions during the manuscript review process.

Appendix A. Supplementary data

Supplementary data to this article can be found online at <https://doi.org/10.1016/j.bmcl.2018.12.045>.

References

- Bravo Y, Bacceti CS, Broadhead A, et al. *Bioorg Med Chem Lett*. 2014;24:2267.
- Stock, N.S.; Chen, A.C.; Bravo, Y.M.; Jacintho, J.D.; Bacceti, J.M.; Stearns, B.A.; Clark, R.C. WO2014/099503 A1.
- Caro P, Kishan AU, Norberg E, et al. *Cancer Cell*. 2012;22:547.
- Aboud OA, Wettersten HI, Weiss RH. *PLoS One*. 2013;8:e71115.
- Schafer ZT, Grassian AR, Song L, Jiang Z, Gerhart-Hines Z, Irie HY, Gao S, Puigserver P, Brugge JS. *Nature*. 2009;461:109 and references cited therein.
- Biswas S, Lunec J, Bartlett K. *Cancer Metastasis Rev*. 2012;31:689.
- Pang T, Kaufman A, Choi J, et al. *Mol Clin Oncol*. 2015;3:308.
- Ito K, Carracedo A, Weiss D, et al. *Nat Med*. 2012;18:1350 and references cited therein.
- Etgen GJ, Mantlo N. *Curr Top Med Chem*. 2003;3:1649–1661.
- Thulasiraman P, McAndrews DJ, Mohiudddin IQ. *BMC Cancer*. 2014;14:724 and references cited therein.
- De Rosa A, Pellegatta S, Rossil M, Tunicl P, Magnoni L, Speranza MC, Malusa F, Miragliotta V, Moril E, Finocchiaro G, Bakker A. *PLoS One*. 2012;7:e52113.
- Zaveri NT, Sato BG, Jiang F, Calaoagan J, Laderoute KR, Murphy BJ. *Cancer Biol Ther*. 2009;8:1252.
- Elikkottil J, Kohli DR, Gupta K. *Cancer Biol Ther*. 2009;8:1262.
- Ham SA, Yoo T, Hwang JS, et al. *Am J Cancer Res*. 2014;4:674.
- Jeong E, Koo JE, Yeon SH, Kwak M-K, Hwang DH, Lee JY. *Mol Carcinog*. 2014;53:926.
- Apostoli AJ, Nicol CJB. *PPAR Res*. 2012;2012:504918.
- Pirat C, Farce A, Lebègue N, et al. *J Med Chem*. 2012;55:4027.
- Pfeifer, L.A.; Ma, T.; Mantlo, N.B.; Michael, L.F.; Mokube, F.M.; Montrose-Rafizadeh, C. U.S. Patent 2010/0099725.
- The screening of test compounds for activities against human PPAR α and PPAR δ receptors were analyzed using commercial kits, Human PPAR α and δ Reporter Assay Systems (Indigo Biosciences, Cat. #IB00111 and IB00121). PPAR α and PPAR δ Reporter cells were dispensed into 96-well assay plates and test compounds were then immediately added to the wells. For the separate antagonist assays, PPAR α agonist GW7647 (20 nM) and PPAR δ agonist GW0742 (3.3 nM) were also added. Following an overnight incubation, the treatment media was discarded and Luciferase Detection Reagent (LDR) added. The luminescence intensity of light emission from the ensuing luciferase reaction is directly proportional to the relative level of PPAR α and δ activation in the reporter cells. Luminescence was read using a Molecular Devices FlexStation 3.
- Female C57BL/6 mice, 6-7 weeks old, were treated with compound 11 at 10 and 30mg/kg. Compound 11 was formulated in .5% methylcellulose to yield a dosing volume of 10 ml/kg and given 2 times per day for 3 consecutive days. A final dose was given in the morning of day 4 and animals were sacrificed 4 hours post last dose. Prior to sacrifice, mice were fasted for 48 hours beginning on day 2. Livers were collected and RNA prepared using Qiazol and RNeasy RNA extraction kit and cDNA was prepared using BioRad iScript cDNA synthesis kit (catalog #170-8891) according to the manufacturer's protocols. Finally gene expression was quantitated using ABI Fast Advanced Master Mix (catalog #4444554) and predesigned primer probe sets from IDT were used to evaluate gene expression changes. Data were normalized to HPRT housekeeping gene.
- Mason JA, Hagel KR, Hawk MA, Schafer ZT. *Trends Cancer*. 2017;3:475.
- B16F10 experimental metastasis model: On day 0, female C57BL/6N mice were injected intravenously with 50,000 B16F10 cells. Beginning on day 1, mice were orally gavaged twice daily with either 11 (30 mg/kg) or vehicle control (0.5% methocel). On day 21, mice were euthanized with isoflurane inhalation. Lungs were removed and placed into 5 ml Fekete's solution. After at least 24 hours in Fekete's solution, pulmonary nodules were enumerated. Nodules were scored according to size using the following formula: Total score = 1a + 2b + 3c where R = diameter of tumor nodule and a = number of nodules with R < 1mm, b = number of nodules where 1 mm \leq R < 2 mm and c = number of nodules with R \geq 2 mm.
- Nieman KM, Kenny HA, Penicka CV, et al. *Nat Med*. 2011;17:1498.
- SKOV-3 experimental xenograft model: Female athymic Fox1 nude mice were implanted with 2e6 SKOV-3 cells in a 1:1 mixture of SKOV-3 cells: matrigel. Cells were injected subcutaneously into the left hind flank. Tumors were measured with calipers and tumor volumes calculated using the formula: tumor volume = (length x width²)/ 2. When tumor volumes were \geq 60 mm³, mice were randomized into groups and treatment with either vehicle (0.5% methocel PO, bid) or 11 (30 mg/kg PO, bid) was initiated. Tumor volumes were determined twice weekly until study termination.